Medicinal Chemistry Research (2019) 28:1601–1617
https://doi.org/10.1007/s00044-019-02397-3

MEDICINAL CHEMISTRY RESEARCH

ORIGINAL RESEARCH

Check for updates

Synthesis, antimicrobial evaluation, and molecular docking of some new angular allylbenzochromone derivatives

El-Sayed I. El-Desoky[1] · Aya A. El-Sawi[1] · Mohamed A. Abozeid[1] · Mohamed Abdelmoteleb[2,3] · Mona Shaaban[4] · Eman M. Keshk[1] · Abdel-Rahman H. Abdel-Rahman[1]

Received: 4 May 2019 / Accepted: 9 July 2019 / Published online: 17 July 2019

Abstract

Different classes of antimicrobial compounds such as *β*-lactams, sulfonamides, aminoglycosides, tetracyclines, quinolines and others have been developed during the 20th century to control the growing antimicrobial resistance. Therefore, there is an urgent need to build up new and effective antimicrobial agents with different working mechanisms to suppress this resistance. Accordingly, the judicious design of antimicrobial organic compounds with antiquorum-sensing activities could be a major solution for this global challenge. Herein, the versatile precursor 6-allyl-3-formyl-4*H*-benzo[*h*]chromen-4-one (**2**) was used for the synthesis of various isolated and condensed naphthoyl or (chromenyl) nicotinonitriles, azalactone, thiazolidinone, xanthene, indenopyridine, Schiff bases, diazepine, imidazole and triazolopyrimidine derivatives **5**-**21** *via* its reactions with several active carbon nucleophiles in addition to amines, benzil and hydrazine. Some of the newly synthesized compounds showed moderately and good antimicrobial activities. The compounds **2** and **14** were the best concerning effects. In addition, the antiquorum-sensing activities of the newly prepared compounds were assessed against *Chromobacterium violaceum*. Specifically, pharmaceutical evaluation, antimicrobial prediction, and molecular docking using computational tools illustrated that the complexes of the latter compounds may show substantial antimicrobial activity in comparison with the other derivatives.

Graphical Abstract

New angular allylbenzochromones were synthesized, and their antimicrobial plus antiquorum-sensing activities were evaluated to give 3-formylchrmone **2** and tetracarbonyl **14** as the best antimicrobials. Computational prediction of pharmacokinetics, drug-likeness properties, biological activity, and molecular docking suggested that formyl chromone **2** and tetracarbonyl **14** may be potent antimicrobial drugs.

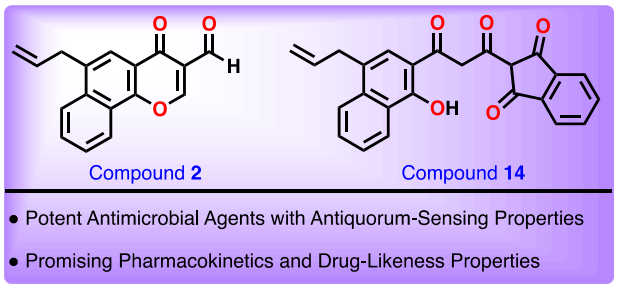

Keywords Chromone · Naphthyl · Antimicrobial activity · Antiquorum-sensing · Docking

✉ El-Sayed I. El-Desoky
prof.desoky.orgchem@gmail.com

[1] Department of Chemistry, Faculty of Science, Mansoura University, El-Gomhoria St, Mansoura 35516, Egypt

[2] Food Allergy Research & Resource Program (FARRP), Department of Food Science & Technology, University of Nebraska, Lincoln, NE, USA

[3] Department of Botany, Faculty of Science, Mansoura University, Mansoura 35516, Egypt

[4] Department of Microbiology, Faculty of Pharmacy, Mansoura University, Mansoura 35516, Egypt

Introduction

Antimicrobial resistance is considered as one of the most serious health problems in the world (Karad et al. 2017; Sapariya et al. 2017). Currently, the presence of numerous resistant microbes leads to continuous demand for the new antimicrobial drugs (Thakkar et al. 2017). Therefore, new strategies are highly required in order to build up new generations of the future antimicrobial agents. In this regard, quorum sensing (QS) is a signaling pathway used by bacteria to control the expression of virulence factors as well as antibiotic resistance. Targeting this signaling system is one of the prominent anti-virulence routes that promises a lower risk of resistance development. In the present time, many medicinal chemists deeply considered the QS signaling system to design new antimicrobial compounds with high efficacy (Abdel-Rahman et al. 2017).

On the other hand, naphthalene is very common moiety in different antimicrobial compounds such as nafcillin, tolnaftate and naftifine (Fig. 1) (El-Desoky et al. 2018). Moreover, in the view of various biologically active chromones (Ellis 1977; Risitano et al. 2001; Yahiaoui et al. 2008), herein we disclose our findings in the design of new molecules bearing chromone as well as naphtalene moities in one hybrid skeleton to be potent antimicrobial agents with antiquorum sensing.

Materials and methods

General

The measurement of melting points was performed on a Gallenkamp apparatus using an open glass capillaries technique. The IR spectra were recorded on a Perkin Elmer Infrared Spectrophotometer Model 157 using potassium bromide discs. The 1H-NMR spectra were recorded on Bruker AC 300 MHz Spectrophotometer or a JOEL 500 MHz spectrophotometer using tetramethylsilane as an internal standard. The NMR solvents were deuterated chloroform ($CDCl_3$) or Dimethylsulfoxide (DMSO-d6), and chemical shifts (δ) were recorded in part per million (ppm). Mass spectra (MS) were determined at 70 eV on a kratos MS or a Varian MAT 311 a spectrometers. Elemental analyses were carried out at the microanalytical center at Cairo University, Egypt. The antimicrobial study of the synthesized compounds was assessed against different organisms such as: *Bacillus cereus* UW85, *Staphylococcus aureus* ATCC 29213, *Escherichia coli* ATCC 12435, *Pseudomonas aeruginosa* PAO1, *Candida albicans* CS351 and *Aspergillus fumigates* 293. The synthesized compounds were completely inactive against *S. aureus* ATCC, *E. coli* ATCC 12435 and *P. aeruginosa* PAO1. *Chromobacterium violaceum* ATCC 12472 was used for detection of quorum sensing inhibition activity (Kindly provided from Prof. Bob Mclean, Department of Biology, Texas State University, USA). All bacterial strains were propagated in Luriae Bertani (LB) media (1% tryptone, 0.5% yeast extract (Bacto-agar, BD Difco), and 1.0% NaCl solidified with 1.5% agar). Saboured's media (BD Difco) was used for assay of antifungal activity against *C. albicans* and for cultures of *A. fumigates*. Ampicillin/clavulanic acid (EPICO Company) and fluconazole (Pfizer Company) were used as antibacterial and antifungal standards, respectively. The PyMOL molecular graphics system, version 2.0 Schrödinger, LLC was used to transfer the structure of ligand and its complexes in PDB format.

Synthesis

Synthesis of 6-allyl-4-oxo-4*H*-benzo[*h*]chromene-3-carboxaldehyde (2)

To a stirred solution of 2-acetyl-4-allyl-1-naphthol (**1**) (5 mmol, 1.13 g) in dimethylformamide (20 ml), phosphorous oxychloride (22 eq., 110 mmol, 10 ml) was added dropwise at −5 °C within 10 min. The mixture was stirred at room temperature for 14 h followed by quenching with cold water and neutralized by adding sodium acetate. The resulting precipitate was collected by filtration, washed with water and recrystallized from ethanol to give pure **2**. Yellowish green needles. Yield = 87%; MP = 73 °C; IR (KBr): ν/cm^{-1} = 3065 (CH, formyl), 1694 (CO, formyl), 1646 (CO, chromone), 1643 (C=C–CO), 1595, 1562 (Ar); ^1H NMR ($CDCl_3$, 500 MHz) δ (ppm): 3.90 (d, 2H, $CH_2CH{=}CH_2$, J = 6.15 Hz), 5.12 (d, 1H, $CH_2CH{=}CH_a$, J = 16.80 Hz), 5.17 (d, 1H, $CH_2CH{=}CH_b$, J = 9.95 Hz), 6.11 (m, 1H, $CH_2CH{=}CH_2$), 7.73 (dd, 1H, H-8, J = 8.45, 7.65 Hz), 7.78 (dd, 1H, H-9, J = 8.45, 7.65 Hz), 8.07 (s, 1H, H-5), 8.13 (d, 1H, H-7, J = 8.45 Hz), 8.54 (d, 1H, H-10, J = 8.45 Hz), 8.71 (s, 1H, H-2), 10.47 (s, 1H, CHO); anal.

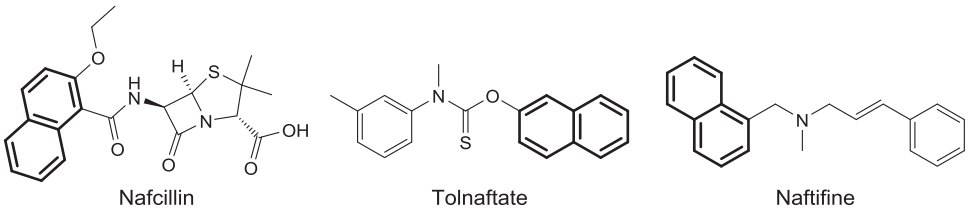

Fig. 1 Naphthyl substituted antimicrobial drugs

calcd for $C_{17}H_{12}O_3$ (264.28): C, 77.26; H, 4.58%. Found: C, 77.43; H, 4.46%.

Reaction of 2 with malononitrile or ethylcyanoacetate

A mixture of compound **2** (5 mmol, 1.32 g), malononitrile (5 mmol, 0.33 g) or ethylcyanoacetate (5 mmol, 0.60 ml) and ammonium acetate (5 g) was refluxed in glacial acetic acid (15 ml) for 5–8 h (TLC control). After cooling to room temperature, the reaction mixture was poured on crashed ice. The solid was filtered off, washed with water, dried, and recrystallized from ethanol to give compounds **5** and **6**.

2-Amino-5-(4-allyl-1-hydroxy-2-naphthoyl)nicotinonitrile (5) Yellow crystals; yield = 77%; MP = 124–126 °C; IR (KBr): ν/cm^{-1} = 3550–3210 (OH), 3343, 3438 (NH2), 2221 (CN), 1620 (CO), 1601 (C=N), 1577 (Ar); ^{1}H NMR ($CDCl_3$, 300 MHz) δ (ppm): 3.71 (d, 2H, $CH_2CH{=}CH_2$, J = 5.70 Hz), 5.08 (d, 1H, $CH_2CH{=}CH_a$, J = 18.30 Hz), 5.13 (d, 1H, $CH_2CH{=}CH_b$, J = 11.10 Hz), 5.82 (brs, 2H, NH_2), 6.09 (m, 1H, $CH_2CH{=}CH_2$), 7.32 (s,1H, H-3), 7.59 (dd, 1H, H-6, J = 7.11, 7.74 Hz), 7.72 (dd, 1H, H-7, J = 7.23, 7.76 Hz), 7.96 (d, 1H, H-5, J = 8.10 Hz), 8.19 (s, 1H, H-4′, pyridine), 8.55 (d, 1H, H-8, J = 8.10 Hz), 8.69 (s, 1H, H-6′, pyridine), 13.45 (s, 1H, OH); MS m/z (%) = 329 [M^+] (40.28), 210 (100.00), 182 (67.28), 164 (20.55), 153 (87.80), 141 (21.65), 128 (43.43), 119 (14.86), 101 (14.52), 91 (23.25), 77 (19.12), 57 (21.05); anal. calcd for $C_{20}H_{15}N_3O_2$ (329.36): C, 72.94; H, 4.59; N, 12.76%. Found; C, 72.86; H, 4.34; N, 12.92%.

5-(4-Allyl-1-hydroxy-2-naphthaoyl)-2-oxo-1,2-dihydropyridine-3-carbonitrile (6) Greenish yellow crystals; yield = 82%; MP = 100–102 °C; IR (KBr): ν/cm^{-1} = 3437 (OH), 3350 (NH), 2214 (CN), 1694, 1644 (CO, amide), 1611 (CO), 1580 (C=C); ^{1}H NMR (DMSO, 400 MHz) δ (ppm): 3.81 (d, 2H, $CH_2CH{=}CH_2$, J = 5.60 Hz), 5.11 (dd, 2H, $CH_2CH{=}CH_2$, J = 9.60 Hz, 11.60 Hz), 6.08 (m, 1H, $CH_2CH{=}CH_2$), 7.46 (s,1H, H-3), 7.58–8.54 (m, 4H, Ar–H), 8.63 (s, 1H, H-4′, pyridine), 8.91 (s, 1H, H-6′, pyridine), 12.16 (brs, 1H, NH), 12.97 (s, 1H, OH); MS m/z (%) = 331 [$M^+ + 1$] (11.49), 330 [M^+] (13.27), 323 (17.95), 305 (7.94), 295 (20.53), 287 (46.65), 270 (23.03), 198 (34.18), 188 (75.58), 172 (100.00), 152 (75.37), 134 (54.87), 120 (46.39), 88 (32.06), 51 (27.06); anal. calcd for $C_{20}H_{14}N_2O_3$ (330.34): C, 72.72; H, 4.27; N, 8.48%. Found: C, 72.69; H, 4.52; N, 8.25%.

Reaction of 2 with N-acetylglycine (aceturic acid) and rhodanine

A mixture of chromone-3-carboxaldehyde derivative **2** (5 mmol, 1.32 g) and the active methylene compound (5 mmol) was refluxed in absolute ethanol (30 ml) in the presence of catalytic amount of triethylamine for 3 h. The reaction mixture was cooled to the room temperature and the formed precipitate was filtered off, washed with cold ethanol several times, dried and recrystallized from ethanol to give pure compounds **7** and **8**.

4-((6-Allyl-4-oxo-4H-benzo[h]chromen-3-yl)methylene)-2-methyloxazol-5(4 H)-one (7) Reddish brown crystals; yield = 80%; MP = 240-242 °C; IR (KBr): ν/cm^{-1} = 1764 (CO, ester), 1639 (CO, chromone), 1621 (C=N), 1508 (Ar); ^{1}H NMR (DMSO, 400 MHz) δ (ppm): 2.31 (s, 3H, CH_3), 3.87 (d, 2H, $CH_2CH{=}CH_2$, J = 7.60 Hz), 5.15 (d, 2H, $CH_2CH{=}CH_2$, J = 16.00 Hz), 6.11 (m, 1H, $CH_2CH{=}CH_2$), 6.59 (s,1H, H-2), 7.50–8.55 (m, 4H, Ar–H), 8.84 (s, 1H, H-5), 8.61 (s, 1H, CH = C–N); anal. calcd for $C_{21}H_{15}NO_4$ (345.35): C, 73.04; H, 4.38; N, 4.06%. Found: C, 73.26; H, 4.24; N, 4.12%.

5-((6-Allyl-4-oxo-4H-benzo[h]chromen-3-yl)methylene)-2-thioxothiazolidin-4-one (8) Pale brown crystals; yield = 82%; MP = 210–212 °C; IR (KBr): ν/cm^{-1} = 3550–3443 (OH, NH), 1708 (CO, chromone), 1642, 1588 (CO, amide), 1551 (Ar), 1195 (CS); MS m/z (%) = 379 [M^+] (59.30), 321 (25.90), 292 (100.00), 246 (25.90), 213 (29.60), 196 (29.60), 175 (25.90), 153 (63.00), 115 (51.90), 98 (33.30), 82 (48.10), 59 (77.80); anal. calcd for $C_{20}H_{13}NO_3S_2$ (379.45): C, 63.3; H, 3.45; N, 3.69%. Found: C, 63.45; H, 3.51; N, 3.54%.

Reaction of 2 with cyclic ketones (cyclopentanone, cyclohexanone, and dimedone)

A mixture of compound **2** (5 mmol, 1.32 g) and cyclic ketone (11 mmol) in absolute ethanol (30 ml) was refluxed for 6–8 h. After cooling to room temperature, the product was precipitated. The precipitated product was filtered off, dried and washed by hot ethanol to give pure products **11a–c**.

6-Allyl-3-(2,3,5,6,7,8-hexahydro-1H-dicyclopenta[b,e]pyran-8-yl)-4H-benzo[h] chromen-4-one (11a) Orange crystals; yield = 75%; MP = 284–286 °C; IR (KBr): ν/cm^{-1} = 2921 (CH, aliphatic), 1641 (C=O, chromone), 1574 (C=C, Ar); ^{1}H NMR (DMSO, 300 MHz) δ (ppm): 2.60–2.80 (m, 8H, 4×CH2, cyclopentane), 3.72 (s, 1H, pyran), 3.91 (d, 2H, $CH_2{=}CHCH_2$), 4.80 (m, 4H, 2×CH2, cyclopentane), 5.20 (m, 2H, $CH_2{=}CHCH_2$), 6.10 (m, 1H, $CH_2{=}CHCH_2$), 7.60–8.81 (m, 7H, ArH); MS m/z (%) = 396 [M^+] (0.39), 332 (22.54), 273 (16.85), 210 (16.66), 185 (100.00), 170 (45.62), 154 (56.60), 141 (69.99), 127 (44.31), 97 (19.18), 83 (62.42), 77 (61.91), 71 (56.96), 58 (48.47); anal. calcd for $C_{27}H_{24}O_3$ (396.49): C, 81.79; H, 6.10%. Found: C, 81.68; H, 6.24%.

6-Allyl-3-(2,3,4,5,6,7,8,9-octahydro-1H-xanthen-9-yl)-4H-benzo[h]chromen-4-one (11b) Pale orange crystals; yield = 78%, MP = 166–168 °C; IR (KBr): $\nu/cm^{-1} = 2972$ (CH, aliphatic), 1643 (C=O, chromone), 1568 (C=C, Ar); ^1H NMR ($CDCl_3$, 300 MHz) δ (ppm): 1.29–1.48 (m, 8H, 4×CH2, cyclohexane), 1.60–1.72 (m, 4H, 2×CH_2 cyclohexane), 3.88 (d, 2H, $CH_2CH{=}CH_2$, $J = 6.30$ Hz), 4.23 (m, 4H, 2×CH2, cyclohexane), 5.12 (d, 1H, CH_2-$CH{=}CH_a$, $J = 16.80$ Hz), 5.16 (d, 1H, $CH_2CH{=}CH_b$, $J = 9.95$ Hz), 6.14 (m, 1H, $CH_2CH{=}CH_2$), 6.52 (d, 1H, H-3, pyran), 7.68-8.06 (m, 4H, H-2, H-5, H-8, H-9), 8.11 (d, 1H, H-7, $J = 7.50$ Hz), 8.53 (d, 1H, H-10, $J = 7.50$ Hz); anal. calcd for $C_{29}H_{28}O_3$ (424.54): C, 82.05; H, 6.65%. Found: C, 82.14; H, 6.52%.

9-(6-Allyl-4-oxo-4H-benzo[h]chromen-3-yl)-3,3,6,6-tetramethyl-3,4,5,6,7,9-hexa-hydro-1H-xanthene-1,8(2H)-dione (11c) Yellow crystals; yield = 82%, MP = 252–254 °C; IR (KBr): $\nu/cm^{-1} = 1721$, 1645 (2×CO xanthene), 1612 (C=C), 1513 (Ar); ^1H NMR ($CDCl_3$, 300 HMz) δ (ppm): 1.02 (s, 6H, 2×CH_3), 1.08 (s, 6H, 2×CH_3), 2.21 (d, 4H, 2×CH_2, $J = 16.20$ Hz), 2.50 (d, 4H, 2×CH_2, $J = 17.40$ Hz), 3.80 (d, 2H, $CH_2CH{=}CH_2$, $J = 6.30$ Hz), 4.59 (s, 1H, CH, pyran), 5.07 (d, 1H, $CH_2CH{=}CH_b$, $J = 16.80$ Hz), 5.11 (d, 1H, $CH_2CH{=}CH_a$, $J = 8.40$ Hz), 6.08 (m, 1H, $CH_2CH{=}CH_2$), 7.67 (m, 2H, H-8, H-9), 7.90 (s, 1H, H-2, pyranone), 8.04 (d, 1H, H-7, $J = 8.40$ Hz), 8.43 (s, 1H, H-5), 8.52 (d, 1H, H-10, $J = 8.40$ Hz). MS m/z (%) = 424 (49.17), 408 (4.01), 396 (4.86), 386 (16.24), 367 (6.17), 274 (100.00), 258 (13.10), 241 (13.62), 226 (9.16), 215 (14.74), 202 (12.99), 188 (6.05), 164 (8.33), 153 (12.28), 128 (12.12), 84 (8.05), 65 (5.10); anal. calcd $C_{33}H_{32}O_5$ (508.61): C, 77.93; H, 6.34%. Found: C, 77.85; H, 6.42%.

Synthesis of 2-((6-allyl-4-oxo-4*H*-benzo[*h*]chromen-3yl) methylene)-1*H*-1,3(2*H*)-dione (12)

Compound **2** (5 mmol, 1.32 g) was refluxed with indandione (5 mmol, 0.73 g) in the presence of few drops of triethyl amine in absolute ethanol (20 ml) for 4 h. After cooling to room temperature, the formed precipitate was filtered off, washed with cold ethanol several times, dried and recrystallized from ethanol to give compound **12**. Yellow crystals; Yield = 88%; MP = 132–134 °C; IR (KBr): $\nu/cm^{-1} = 1725$, 1684 (2×CO cyclopentadione), 1648 (CO chromone), 1621 (C=C), 1587, 1545 (Ar); ^1H NMR (DMSO-d6, 300 Hz) δ (ppm): 3.95 (d, 2H, $CH_2CH{=}CH_2$, $J = 6.91$ Hz), 5.15 (d, 1H, CH_2-$CH{=}CH_a$), 5.19 (d, 1H, $CH_2CH{=}CH_b$), 6.09 (m, 1H, $CH_2CH{=}CH_2$), 7.88-8.04 (m, 9H, H-2, H-7, H-8, H-9, H-10, H-1′, H-2′, H-3′, H-4′), 8.13(s, 1H, H-5), 10.36 (s, 1H, C(CO)CHC(C=O)$_2$); MS m/z (%) = 394 [$M^+ + 2$] (3.20), 393 [$M^+ + 1$] (4.08), 392 [M^+] (3.93), 389 (78.76), 333 (73.47), 306 (26.09), 249 (16.02), 237 (11.44), 208 (13.40), 179 (30.06), 151 (64.05), 124 (66.42), 76 (48.41), 74 (100.00); anal. calcd for $C_{26}H_{16}O_4$ (392.40): C, 79.58; H, 4.11%. Found: C, 79.62; H, 4.01%.

Synthesis of 3-(4-allyl-1-hydroxy-2-naphthoyl)-5*H*-indeno [1,2-*b*]pyridin-5-one (13)

A mixture of compound **2** (5 mmol, 1.32 g), indan-1,3-dione (5 mmol, 0.73 g) and ammonium acetate (2 g) in glacial acetic acid (15 mL) was refluxed for 4–5 h (TLC control). After completion of the reaction, the reaction mixture was poured into crushed ice followed by vigorous stirring. The formed precipitate was filtered off, washed with water, dried, and recrystallized from ethanol to give compound **13**. Gray powder; yield = 74%; MP = 162–164 °C; IR (KBr): $\nu/cm^{-1} = 3550$–3250 (OH), 1724 (CO cyclopentanone), 1627 (CO), 1624 (C=N), 1611 (Ar); ^1H NMR (DMSO-d6, 300 Hz) δ (ppm): 3.72 (d, 2H, $CH_2CH{=}CH_2$, $J = 5.70$ Hz), 5.03 (d, 1H, $CH_2CH{=}CH_a$, $J = 17.30$ Hz), 5.09 (d, 1H, $CH_2CH{=}CH_b$, $J = 9.60$ Hz), 6.01 (m, 1H, $CH_2CH{=}CH_2$), 7.42 (s, 1H, H-5), 7.42–7.97 (m, 6H, H−6, H-7, H-1′′, H-2′′, H-3′′, H-4′′), 8.04 (d, 1H, H-5, $J = 8.10$ Hz), 8.19 (s, 1H, H-2', pyridine), 8.44 (d, 1H, $J = 8.40$ Hz), 8.98 (s, 1H, H-4', pyridine), 12.75 (brs, 1H, OH); MS *m/z* (%) = 393 [$M^+ + 2$] (2.05), 391 [M^+] (1.85), 387 (40.19), 386 (10.42), 347 (4.71), 318 (2.38), 207 (50.56), 179 (64.8), 163 (32.72), 151 (100.00), 150 (64.93), 137 (24.02), 126 (59.83), 75 (36.31), 44 (34.79); anal. calcd For $C_{26}H_{17}NO_3$ (391.42): C, 79, 78; H, 4.38; N, 3.58%. Found: C, 79.83; H, 4.29; N, 3.61%. 4.2.12. 2.4.13%.

Synthesis of 2-(3-(4-allyl-1-hydroxynaphthalen-2-yl)-3-oxopropanoyl)-1*H*-indene-1,3-(2*H*)-dione (14)

A solution of compound **2** (5 mmol, 1.32 g) and indan-1,3-dione (0.073 g, 5 mmol) in ethanol (95%) was refluxed for 30 min. After cooling to room temperature, the precipitate was collected, filtered off, washed with cold ethanol, dried and recrystallized from ethanol to give compound **14**. Pale yellow crystals; yield = 88%, 178–179 °C; IR (KBr): $\nu/cm^{-1} = 3470$–3350 (OH), 1738, 1705, 1645 (3×CO), 1626 (CO, chromone), 1598, 1510 (Ar). 1H NMR (DMSO-d6, 300 Hz) δ (ppm): 2.98 (d, 2H, $COCH_2CO$), 3.84 (s, 1H, indandione), 3.96 (d, 2H, $CH_2CH = CH_2$), 5.17 (d, 1H, CH2CH = CH_a), 5.21 (d, 1H, $CH_2CH{=}CH_b$), 6.09 (m, 1H, $CH_2CH = CH_2$), 7.31–7.92 (m, 3H, H-3, H-6, H-7), 7.95 (s, 4H, H-4′, H-5′, H-6′, H-7′), 8.22 (d, 1H, H-5), 8.38 (d, 1H, H-8). MS *m/z* (%) = 400 [$M^+ + 2$] (3.19), 399 [$M^+ + 1$] (8.10), 398 [M^+] (14.72), 261 (8.8), 211 (10.12), 184 (19.24), 152 (19.7), 127 (16.74), 78 (30.69), 76 (25.55), 63 (34.89), 45 (36.45), 28 (38.01), 15 (100.00); anal. calcd. For

$C_{25}H_{18}O_5$ (398.12): C, 75.37; H, 4.55%. Found: C, 75.42; H, 4.41%.

Reaction of 2 with primary amines

A mixture of compound **2** (5 mmol, 1.32 g) and amine (11 mmol) was refluxed in absolute ethanol (30 ml) for 2 h. After cooling to room temperature, the product was precipitated. The formed precipitate filtered off, washed by ethanol and dried to give compounds **16a–c** and **17**.

6-Allyl-2-(phenylamino)-3-(phenylaminomethylenyl)-2H,4H-benzo[h]chromen-4-one (16a) Yellow crystals; yield = 82%; MP = 116–118 °C; IR (KBr): ν/cm^{-1} = 3439 (NH), 1648 (CO), 1596 (C = N), 1582 (C=C), 1560 (Ar). ^{1}H NMR (DMSO-d6, 300 Hz) δ (ppm): 3.82 (d, 2H, $CH_2CH{=}CH_2$, J = 6.90 Hz), 4.30 (brs, NH, 2° amine, exchangeable with D_2O), 5.11 (d, 1H, $CH_2CH{=}CH_a$, J = 18.80 Hz), 5.15 (d, 1H, $CH_2CH{=}CH_b$, J = 9.90 Hz), 6.13 (m, 1H, $CH_2CH{=}CH_2$), 6.22 (s, 1H, H-2, pyran), 7.29-8.39 (m, 16H, ArH, C–CH = N or C=CH–NH), 11.88 (s, 1H, NH keto-enamine or OH enol-imine, exchangeable with D_2O), 11.92 (s, 1H, NH keto-enamine or OH enol-imine, exchangeable with D_2O); MS m/z (%) = 432 [M^+] (0.05), 340 (7.70), 339 (100.00), 262 (71.94), 236 (35.35), 182 (25.95), 165 (36.35), 152 (56.52), 128 (32.66), 78 (46.38), 57 (61.03); anal. calcd. For $C_{29}H_{24}N_2O_2$ (432.18): C, 80.53; H, 5.59; N, 6.48%. Found: C, 80.39; H, 5.67; N, 6.52%.

6-Allyl-2-((2-methoxyphenyl)amino)-3-((2-methoxyphenyl) aminomethylene)-2H-benzo[h] chromen-4-one (16b) Yellow crystals; yield = 84%; MP = 156–158 °C; IR (KBr): ν/cm^{-1} = 3307 (NH), 1649 (CO), 1599 (C=N), 1584 (C=C), 1556 (Ar); MS m/z (%) = 492 [M^+] (0.05), 491 [$M^+ - 1$] (0.07), 444 (0.16), 429 (0.07), 406 (0.09), 385 (0.44), 372 (0.59), 371 (1.65), 369 (10.95), 354 (100.00), 249 (12.64), 235 (18.68), 182 (14.28), 165 (21.68), 152 (33.44), 139 (12.18), 127 (20.45), 77(24.14), 57 (57.42); anal. calcd. For $C_{31}H_{28}N_2O_4$ (492.57): C, 75.59; H, 5.73; N, 5.69%. Found: C, 75.48; H, 5.84; N, 5.78%.

6-Allyl-2-(pyridin-3-ylamino)-3-(pyridin-3-ylaminomethylene)-2*H*,4*H*-benzo [*h*]chromen-4-one (16c)

Golden yellow crystals; Yield = 80%; MP = 177–178°C; IR (KBr): ν/cm^{-1} = 3600–3200 (NH), 1650 (CO, chromone), 1597 (C=N), 1583 (C=C), 1561 (Ar). ^{1}H NMR (DMSO-d6, 300 Hz) δ (ppm): 3.80 (d, 2H, $CH_2CH{=}CH_2$, J = 6.88 Hz), 4.32 (brs, NH, 2° amine, exchangeable with D_2O), 5.12 (d, 1H, $CH_2CH{=}CH_a$, J = 16.90 Hz), 5.17 (d, 1H, J = 9.70 Hz), 6.08 (m, 1H, CH_2–CH=CH_2), 6.21 (s, 1H, H-2, pyran), 7.40–8.59 (m, 8 H, ArH), 8.67 (s, 1 H, C–CH=N or C=CH–NH), 8.82 (s, 1H, H-2, pyridine), 9.22 (s, 1H, H-2, pyridine), 11.71 (s, 1H, NH keto-enamine or OH enolimine, exchangeable with D_2O), 11.75 (s, 1H, NH keto-enamine or OH enol-imine, exchangeable with D_2O); MS m/z (%) = 434 [M^+] (0.09), 398 (0.56), 379 (2.40), 364 (0.58), 340 (3.62), 321 (8.62), 305 (10.22), 291 (20.34), 262 (12.56), 235 (11.24), 208 (63.90), 192 (33.41), 134 (43.45), 105 (100.00), 78 (73); anal. calcd. For $C_{27}H_{22}N_4O_2$ (434.17): C, 74.64; H, 5.10; N, 12.89%. Found: C, 74.48; H, 5.27; N, 12.95%.

7-Allyl-12-hydroxybenzo[b]benzo[6,7]chromeno[2,3-e][1,4] diazepin-13(5 H)-one (17) Orange crystals; yield = 80%; MP = 242–244 °C; IR (KBr): ν/cm^{-1} = 3423 (NH), 1633 (C=O), 1576 (C=N), 1570 (C=C); ^{1}H NMR (DMSO, 400 Hz) δ (ppm): 3.92 (d, 2H, $CH_2CH{=}CH_2$, J = 6.0 Hz), 5.16 (d, 2H, $CH_2CH{=}CH_a$, J = 13.20 Hz), 6.13 (m, 1H, $CH_2CH{=}CH_2$),7.47 (s, 1H, H-5), 7.81 – 7.90 (m, 6H, ArH), 8.24 (d, 1H, H-10, J = 8.40 Hz), 8.54 (d, 1H, H-7, J = 8.40 Hz), 9.08 (s, 1H, CH = N), 13.62 (brs, 1H, NH); MS m/z (%) = 356 [$M^+ + 4$] (6.46), 354 [$M^+ + 2$] (24.10), 352 [M^+] (95.93), 336 (11.94), 295 (4.25), 210 (7.53), 193 (7.21), 181 (8.04), 165 (22.47), 152 (17.44), 142 (7.74), 127 (14.59), 119 (36.57), 108 (38.48), 78 (74.80), 63 (100.00), 45 (40.94); anal. calcd For $C_{23}H_{16}N_2O_2$ (352.39): C, 78.39; H, 4.58; N, 7.65%. Found: C, 78.23; H, 4.64; N, 7.86%.

Synthesis of 4,5-diphenyl-2-(4-oxo-4H-1-benzo[7,8] benzopyran-3-yl)imidazole (18)

A mixture of compound 2 (2 mmol, 0.53 g), *o*-phenylenediamine or benzil (2 mmol) and ammonium acetate (2 g) was refluxed in glacial acetic acid (15 ml) for 5 h. After cooling to room temperature, the reaction mixture was poured into crushed ice. The precipitate was filtered off, dried, and recrystallized from ethanol/acetone mixture (1:1) to give compound **18**. Golden yellow crystals; yield = 80%; MP = 194 °C; IR (KBr): ν/cm^{-1} = 3348 (NH), 1640 (CO), 1600 (C=C), 1575 (Ar); ^{1}H NMR ($CDCl_3$, 300 Hz) δ (ppm): 3.93 (d, 2H, $CH_2CH{=}CH_2$, J = 6.33 Hz), 5.17 (dd, 1H, $CH_2CH{=}CH_a$, J = 15.90 Hz), 5.22(dd, 1H, $CH_2CH{=}CH_b$, J = 8.70 Hz), 6.16 (m, 1H, $CH_2CH{=}CH_2$), 7.30–7.80 (m, 14H, ArH), 8.10 (s, 1H, H5), 8.14 (d, 1H, H-7, J = 8.40 Hz), 8.65 (d, 1H, J = 8.19 Hz, H-10), 9.75 (brs, 1H, NH); anal. calcd. For $C_{31}H_{22}N_2O_2$ (454.52): C, 81.92; H, 4.88; N, 6.16%. Found: C, 82.02; H, 4.74; N, 6.22%.

Synthesis of 4-(4-allyl-1-hydroxy-2-naphthoyl)-1-phenylpyrazole (19)

A mixture of compound **2** (2 mmol, 0.53 g) and phenylhydrazine (2 mmol, 0.22 g, 2 mL) in absolute ethanol (25 ml) was refluxed for 5 h. The solvent was concentrated to 10 ml, diluted with water/conc. HCl mixture (10 ml/1 ml) and left

to cool. The solid was formed, filtered off, dried, and recrystallized from ethanol to give compound **19**. Gray crystals; yield = 65%; MP = 110 °C; IR (KBr): ν/cm^{-1} = 3310–3530 (OH), 3430 (NH), 1635 (CO), 1601 (Ar); 1 H NMR ($CDCl_3$, 300 MHz) δ (ppm): 3.95(d, 2H, $CH_2CH{=}CH_2$, J = 6.90 Hz), 4.97 (dd, 1H, $CH_2CH{=}CH_b$, J = 16.80 Hz), 5.03 (dd, 1H, $CH_2CH{=}CH_a$, J = 9.60 Hz), 6.02 (m, 1H, $CH_2CH = CH_2$), 7.01–8.19 (m, 12H, ArH), 13.92 (s, 1H, OH, exchangeable with D_2O); MS m/z (%) = 354 [M^+] (21.01), 339 (10.20), 326 (86.12), 315 (2.66), 300 (51.64), 282 (25.39), 256 (28.33), 243 (34.58), 226 (16.50), 209 (33.84), 188 (16.71), 171 (20.88), 153 (38.37), 140 (16.17), 127 (18.22), 113 (25.40), 103 (44.10), 91 (55.99), 77 (100.00); anal. calcd. For $C_{23}H_{18}N_2O_2$ (354.4): C, 77.95; H, 5.12; N, 7.90%. Found: C, 77.82; H, 5.07; N, 8.11%.

Reaction of 3 with 3-aminotriazole: synthesis of 20a,b

A mixture of compound **2** (2.5 mmol, 0.66 g) and 3-aminotriazole (2.5 mmol, 0.21 g) was refluxed in absolute ethanol (30 ml) for 3 h. After cooling to room temperature, the precipitate filtered off, washed with ethanol and recrystallized to give compound **20a,b**. Golden yellow crystals; yield = 70%, MP = 192 °C; IR (KBr): ν/cm^{-1} = 3448 (NH), 1667 (CO), 1620 (C=N), 1577 (C=N), 1530 (C=C); ^{1}H NMR (DMSO-d6) (300 Hz) δ (ppm): 3.79 (d, 2H, $CH_2CH{=}CH_2$, J = 6.00 Hz), 5.09 (dd, 1H, $CH_2CH{=}CH_b$, J = 13.80 Hz), 5.13 (d, 1H, $CH_2CH{=}CH_a$, J = 6.60 Hz), 6.07 (m, 1 H, $CH_2CH{=}CH_2$), 7.64-8.32 (m, 8H, ArH), 12.10 (brs, 1H, NH); MS m/z (%) = 330[M^+] (100.00), 289 (2.44), 210(55.12), 182(64.2), 165(21.06), 153(52.48), 147(10.4), 127(25.98), 120(9.19), 115(9.9), 92 (26.32), 76(29.61), 58(24.47); anal. calcd For $C_{19}H_{14}N_4O_2$ (330.35): C, 69.08; H, 4.27; N, 16.96%. Found: C, 69.14; H, 4.34; N, 17.12%.

Reaction of 20a,b with triethylamine: synthesis of 21a,b

Refluxing a solution of compound **20a,b** (1 mmol, 0.33 g) and triethylamine (0.5 ml) in absolute ethanol (10 ml) for 3 h. The reaction mixture was evaporated under vacuum and the remaining residues were purified using column chromatography (petroleum ether/ethyl acetate = 8:2) to give the products **21a,b** (Inseparable mixture). Yellow powder; yield = 70%; MP = 142–144 °C; IR (KBr): ν/cm^{-1} = 3480–3300 (OH), 1670 (CO), 1605 (C=C), 1560 (Ar). ^{1}H NMR (DMSO-d6) (300 Hz) δ (ppm): 3.81 (d, 2 H, $CH_2CH{=}CH_2$), 5.07–5.14 (m, 2 H, $CH_2CH{=}CH_2$), 6.14 (m, 1H, $CH_2CH{=}CH_2$), 7.60–8.65 (m, 5H, ArH), 9.1 (s, 2H, pyrimidine), 9.48 (s, 1H, triazole, 21a), 9.51 (s, 1H, triazole, 21b); anal. calcd. For $C_{19}H_{14}N_4O_2$ (330.35): C, 69.08; H, 4.27; N, 16.96%. Found: C, 69.02; H, 4.39; N, 16.91%.

Evaluation of the antimicrobial and antiquorum-sensing activities

Screening of antimicrobial activity

Antibacterial effect of the synthesized compounds was performed using the agar plate diffusion method. The tested micro-organisms were propagated in Muller Hinton (MH) media at 37 °C for 24 h. The Melted MH media at 50 °C was inoculated with 20 µL of 1×10^6 CFU/mL of the tested microorganisms, mixed well and poured into 9-cm-diameter plates and left to solidify. Wells were cut into agar plates and the tested compounds dissolved in DMSO to get a concentration of 5 mg/mL and 100 µL was added to the corresponding wells. The compounds are allowed to diffuse for 2 h at 4 °C and incubated at 37 °C for 24 h in the assessment of antibacterial and antifungal activities. While, for *Aspergillus fumigatus* the plates were incubated for 72 h at 37 °C. In each plate, a well containing DMSO was also included as a negative control. The diameter of inhibition zone was measured in millimeter and the activity of the tested compounds was estimated in comparison to ampicillin/clavulanic acid and fluconazole and amphotericin B as reference antibacterial and antifungal drugs, respectively (Performance standards 2015).

Quorum-sensing inhibitory activity

The quorum sensing reporter strain *C. violaceum* ATCC 12472 was cultivated in LB broth for 48 h at 28 °C. LB agar plates were prepared and left to complete solidification, *C. violaceum* was inoculated (50 µL/plate) in 5 mL soft LB agar and poured on the prepared LB agar plates. Wells were made and 100 µL of the tested compounds (5 mg/mL) was added to each well. Well containing DMSO was also included as negative controls and wells containing catechin (5 mg/mL) was also included as positive controls. Plates were incubated at 28 °C for 48 h, *C. violaceum* growth appears as violet pigment and the quorum sensing inhibiting activity was detected as inhibition of pigment formation around the wells. Bacterial growth inhibition would result in a clear zone. Bacterial growth inhibition was measured as radius ($r1$) in mm, while both growth and pigment inhibition was measured as radius ($r2$) in mm. The pigment inhibition (QS inhibition) was determined by subtracting bacterial growth inhibition ($r1$) from the total radius ($r2$); thus, QS inhibition = ($r2-r1$) in mm (McClean et al. 1997, 2004).

Determination of minimal inhibitory concentrations (MICs)

The investigated compounds were assessed for in vitro antibacterial efficacy as reported by CLSI, 2015 and for

in vitro antifungal activity according the CLSI M27-A3 and CLSI M38-A2 methods (CLSI 2008). In brief, twofold serial dilutions of the active compounds were prepared in 0.1 mL MH broth for antibacterial and yeast peptone dextrose for antifungal assay. Each well was inoculated with 0.01 of the diluted bacterial suspension (5 × 106 CFU/mL). The antimicrobial activity of ampicillin/clavulanic aicd, fluconazole and amphotericin B was estimated and used as a positive control. The microtiter plates were incubated at 37 °C for 18 h. The MIC was detected to the lowest concentration that inhibited visible microbial growth (Reference method M27-A3 2008; Reference method M38-A2 2008).

Computational analysis

Estimation of the pharmacokinetic parameters

Pharmacokinetics and drug-likeness prediction for the synthesized compounds were performed by online tool SwissADME predictor software (http://www.swissadme.ch/index.php) made by Swiss Institute of Bioinformatics (http://www.sib.swiss). Chemical 2D structures of the molecules were drawn using Marvin Sketch (ChemAxon, Version 18.30) and converted into SMILEY mode by online SMILES translator available in SwissADME predictor software. In the present study, absorption, distribution, metabolism, excretion and toxicity (ADMET) behaviors of the synthesized compounds were calculated by using SwissADME predictor and AdmetSAR-2.0 online software (http://lmmd.ecust.edu.cn/admetsar2) by introducing the SMILEYS mode of synthesized compounds (Daina et al. 2017; Yang et al. 2018).

Prediction of antimicrobial activity using PASS online predictor

Prediction of activity spectra for substance (PASS) (http://www.pharmaexpert.ru/passonline/predict.php) is one of the frequently used online software in the drug innovation and development environment. This tool is used to predict the 3678 type of pharmacological effects based on the decomposition of the structure and interpretation of the biological active spectra using the SMILEYS structure of molecules. Furthermore, it determines the most probable biological activity among the compounds from the viable database. In this study, the antibacterial and antifungal potential of the synthesized derivatives was predicted. Pa (Probability of being active) and Pi (Probability of being inactive) values were given by the PASS online software for antibacterial and antifungal activities (Parasuraman 2011).

Molecular docking analysis

The binding modes of the most two active antimicrobial compounds (**2** and **14**) were determined using in silico molecular docking simulation. Chemical structures of ligands were drawn into Marvin Sketch (ChemAxon) and the most energetically favored conformer was saved as (*.sdf) file format for docking. To predict the inhibition mechanisms and the most suitable targets for the synthesized derivatives, several biological targets related to antibacterial and antifungal activities among the studied species were used. In addition to PDB models for these targets in *B. cereus*, *C. albicans*, *A. fumigatus*, highly similar homologs PDB models in closely related species were used. *Bacillus halodurans* penicillin binding protein (PDB ID 3TG9), *B. cereus D*-alanyl Carrier Protein Ligase DltA (PDB ID 3FCE), *B. cereus* DNA glycosylase AlkD (PDB ID 5KUB) as antibacterial protein targets, and lanosterol 14-*alpha* demethylase from *Saccharomyces cerevisiae* (PDB ID 4LXJ), *C. albicans* (PDB ID 5TZ1), and *A fumigatus* (PDB ID 4UYL) in addition to beta-1,3-glucanase from *C. albicans* (PDB ID 3N9K) as antifungal targets were selected and fetched from Protein Data Bank (www.rcsb.org/pdb). Molecular Auto Dock 4.2 (MGL tools-1.5.6) docking protocol was performed using PYRX software (Trott, Olson 2010). Polar hydrogen atoms were added, nonpolar hydrogen atoms were merged, and Gasteiger partial atomic charges then were assigned to the derivatives. All rotatable bonds were allowed to rotate during the docking process, and then protein–ligand interactions were saved in the Protein Data Bank, Partial Charge and Atom Type (PDBQT) format suitable for calculating binding energy. The structure of ligand and its complexes were transformed into PDB file format using PYMOL software (Version 2.2.3). Docking results were visualized using PYMOL for 3TG9 and 4LXJ. After docking, the best interactions were analyzed to figure out the antifungal and antibacterial inhibitor by visualizing the hydrophobic and electrostatic interactions of derivatives within the binding pocket of target proteins.

Results and discussion

Chemistry

The precursor 6-allyl-3-formyl-4*H*-benzo[*h*]chromone (**2**) was synthesized *via* Vilsmeier–Haack reaction of the previously prepared 4-allyl-1-hydroxy-2-acetonaphthone (**1**) as shown in Scheme 1 (El-Desoky et al. 2018). The Knoevengel reaction of formylchromone **2** with the carbon nucleophiles precursors such as malononitrile and ethyl

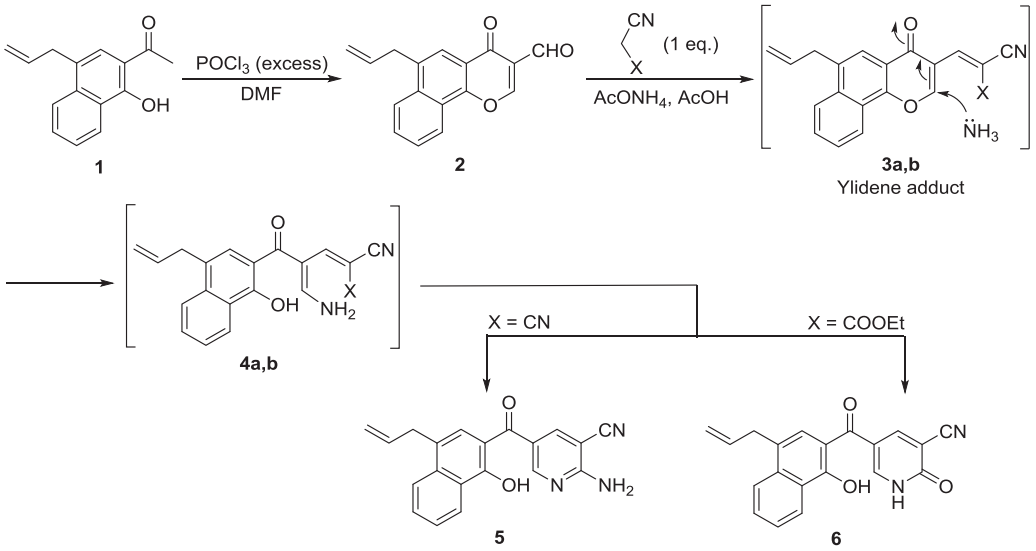

Scheme 1 Synthesis of naphthoyl nicotinonitriles **5** and **6**

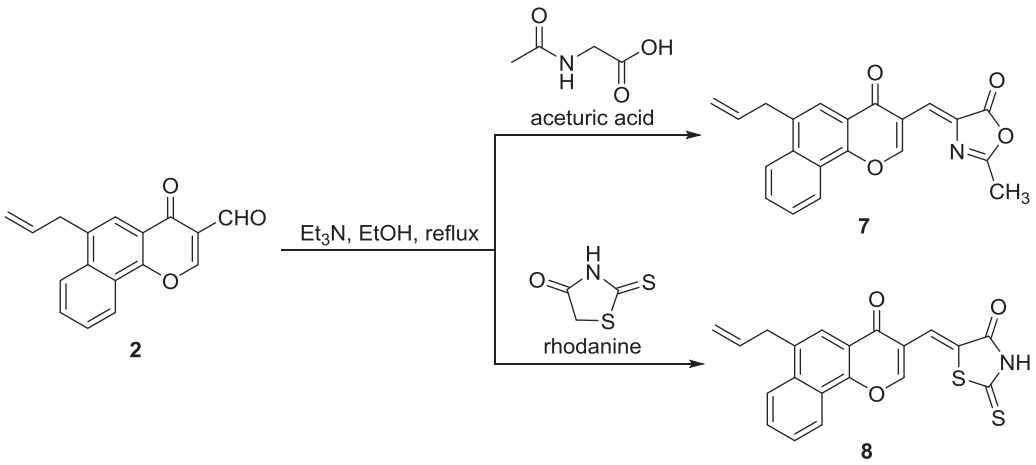

Scheme 2 Synthesis of azalactone **7** and thioxothiazolidinone **8**

cyanoacetate in the presence of ammonium acetate afforded the corresponding 2-amino-5-(4-allyl-1-hydroxy-2-naphthoyl)nicotinonitrile **(5)** and 5-(4-allyl-1-hydroxy-2-naphthoyl)-2-oxo-1,2-dihydropyridine-3-carbonitrile **(6)**, respectively (Scheme 1). The reaction mechanism involves the formation of the ylidene intermediates **3a,b** followed by aminolysis of the pyrone ring to give the intermediates **4a,b**, subsequently the nucleophilic attack of the amino group to C≡N or COOEt groups yielded the final naphthoyl nicotinonitriles **5** and **6**, respectively.

The reaction of formylchromone **2** with active methylene compounds such as *N*-acetylglycine (aceturic acid) and rhodanine gave the corresponding azalactone **7** and thioxothiazolidinone derivatives **8**, respectively (Scheme 2).

Also, condensation of 3-formylchromone **2** with active methylene partners namely; cyclopentanone, cyclohexanone, and dimedone in the presence of triethylamine afforded the corresponding dicyclopenta[*b,e*]pyran and benzochromenyl xanthene derivatives **11a–c** (Scheme 3). This process involves domino approach, firstly nucleophilic condensation of the cyclic ketone giving ylidines **9a–c** which afford intermediates **10a–c** *via* Michael addition of a second molecule of the cyclic ketone, and finally intramolecular cyclodehydration gave products **11a–c**.

On the other hand, condensation of 3-formylchromone **2** with indandione in the presence of triethylamine gave the monoadduct **12** regardless the stoichiometric ratio (Scheme 4). Moreover, refluxing of 3-formylchromone **2** with indandione in the presence of ammonium acetate and acetic acid afforded naphthoyl indenopyridinone derivative **13**. The same product **13** could also be prepared from the monoadduct **12** by refluxing in the presence of $AcONH_4$/AcOH which support

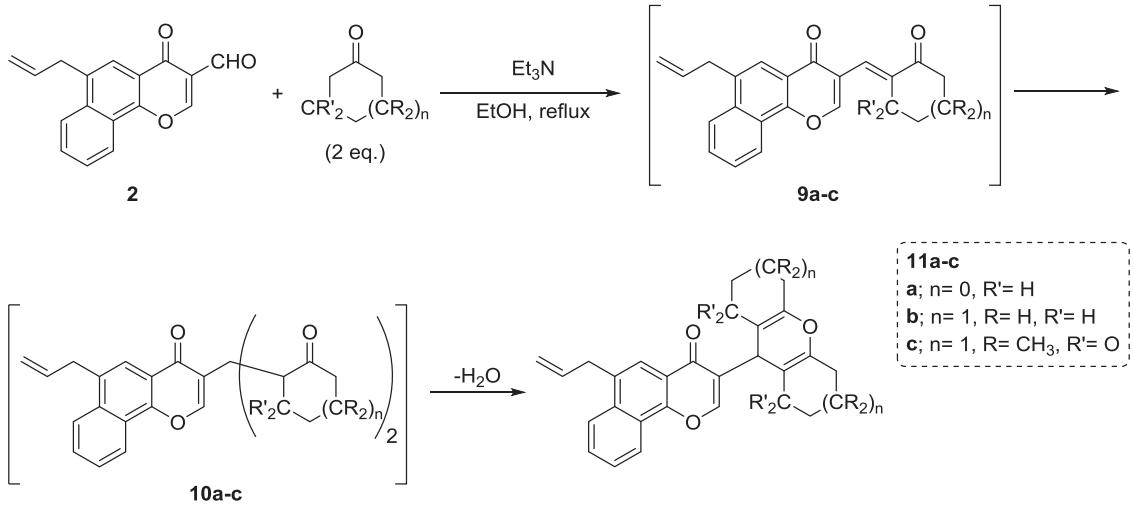

Scheme 3 Reaction of formylchromone **2** with cyclopentanone, cyclohexanone, and dimedone

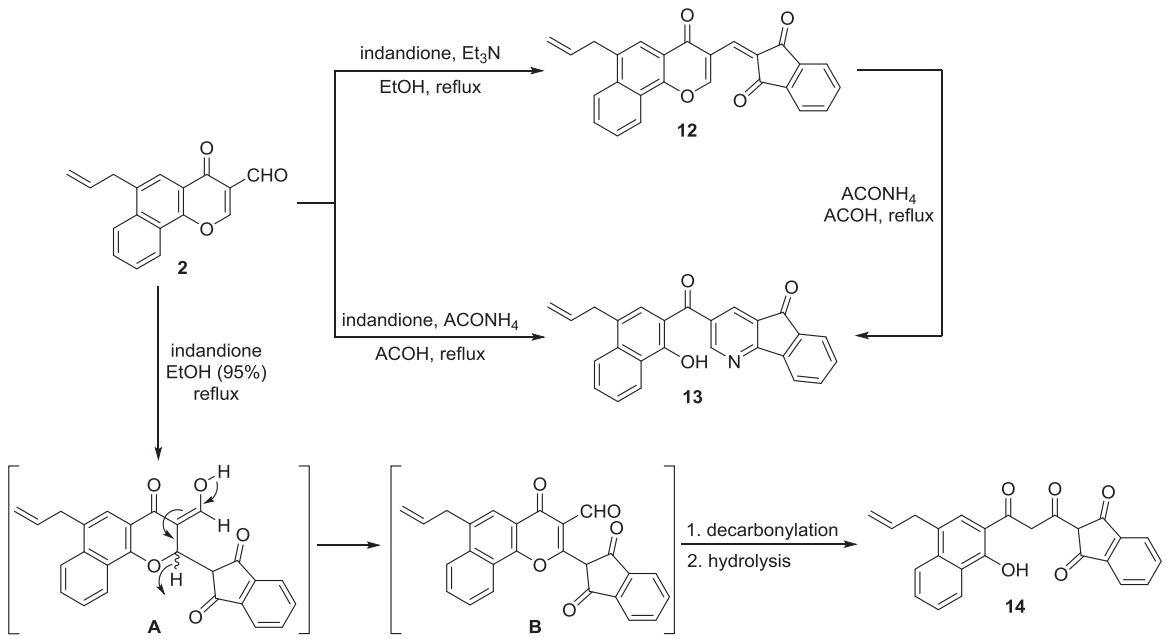

Scheme 4 Reaction of formylchromone **2** with indandione

the intermediacy of monoadduct **12** in the direct synthesis of indenopyridinone **13** from 3-formylchromone **2**. In completely different scenario, refluxing of 3-formylchromone **2** with indandione in ethanol (95%) in the absence of basic catalyst afforded the unexpected tetracarbonyl derivative **14** (Scheme 4). The suggested mechanism depends upon firstly 1,4-Michael addition of indandione molecule to give the intermediate (**A**) followed by dehydrogenation affording the intermediate (**B**) which underwent decarbonylation (Ghosh and Khan 1981; Sigg et al. 1982) and subsequently hydrolysis of pyrone ring to form product **14**.

Condensation of 3-formyl benzo[*h*]chromone **2** with alcoholic solution of primary amines such as aniline, *o*-anisidine and 3-aminopyridine gave the corresponding products **16a–c** in about 80% yields (Scheme 5). Firstly, formylchromone **2** reacted with one equivalent of amine to give the intermediate anils **15a–c** which overreacted in situ with the second equivalent of amine *via* 1,4-nucleophilic addition affording the desired products keto-enamine, **16a–c** which present in tautomerism with their enol-imines, **16a–c** (Rodríguez et al. 2007).

The reaction of formylchromone **2** with *o*-phenylenediamine afforded diazepine **17** as shown in Scheme 6. In addition, mixing of the precursor **2** with benzil in the presence of ammonium acetate and acetic acid yielded the imidazole containing heterocyclic compound **18** in very

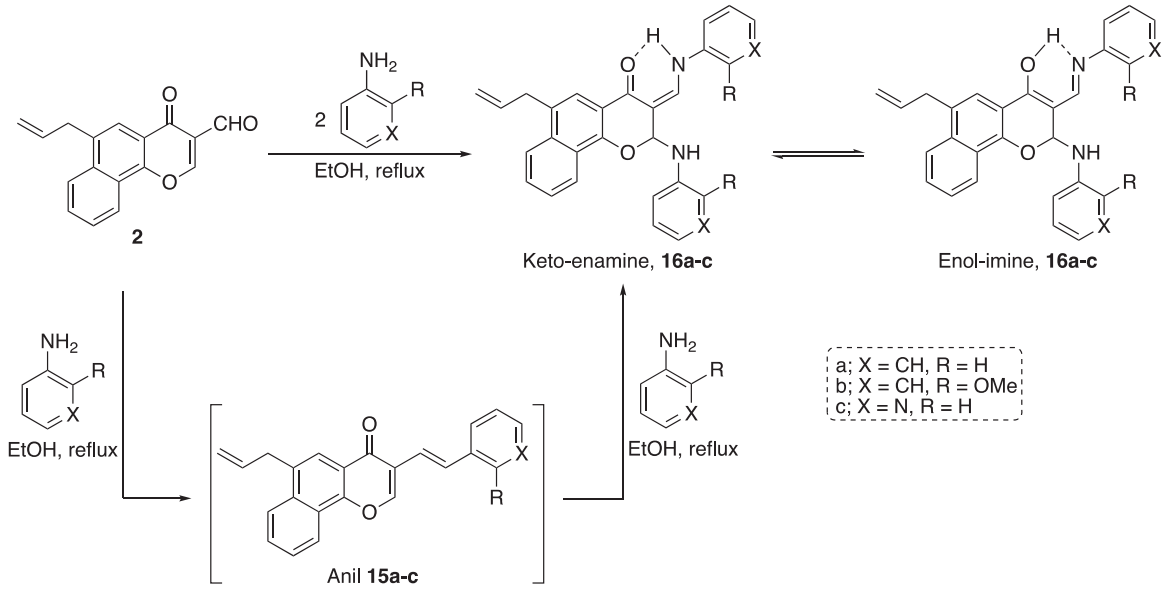

Scheme 5 Condensation of formylchromone **2** with primary amines

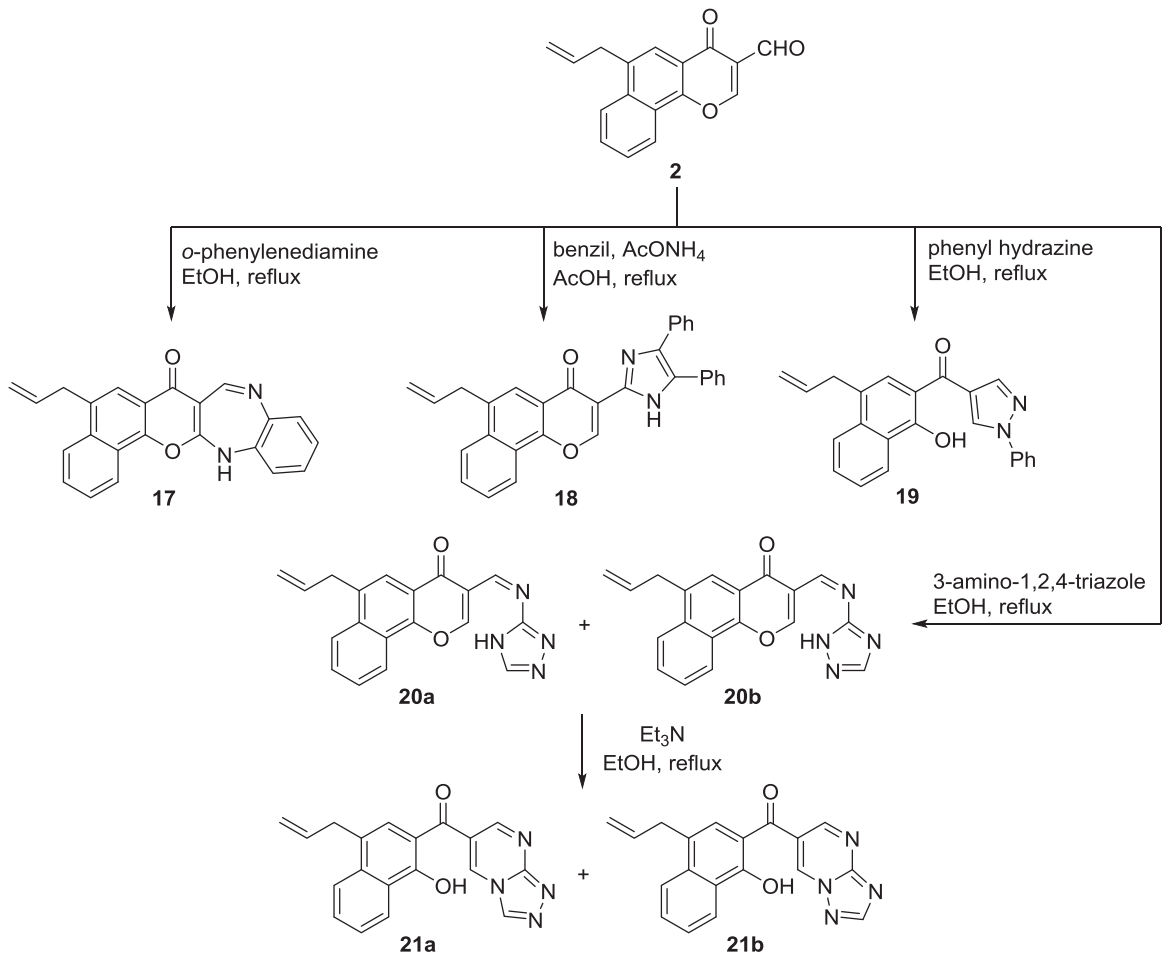

Scheme 6 Reactions of formylchromone **2** with *o*-phenylenediamine, benzil, phenylhydrazine and 3-amino-1,2,4-triazole

good yield. The reaction of formylchromone **2** with phenylhydrazine as bifunctional nucleophile afforded the corresponding pyrazole derivative **19**. This domino reaction included the in situ generation of hydrazone intermediate followed by the intramolecular attack at the electrophilic chromone C-2 by the second nucleophilic NH functionality. Similarly, condensation of 3-amino-1,2,4-triazole with formylchromone **2** yielded the corresponding anils **20a,b** (tautomeric mixture) in 70% yield (Scheme 6). The presence of two close and reactive functionalities (i) The electrophilic C-2 in the chromone ring (ii) The nucleophilic amine in the triazolyl moiety pushed the second step from anil **20a,b** to the non-separable triazolopyrimidines **21a,b** in the presence of catalytic amount of triethyl amine.

The ^{1}H NMR spectra showed clearly the signals both of isomers **21a,b** (1:1 ratio). For instance, the two singlets at δ 9.51, 9.48 ppm were assigned as the triazolyl protons in both isomers **21a,b**. By considering the chemical environment in both isomers **21a,b**, the singlet at 9.48 ppm was assigned for the triazolyl protons of isomer **21a** because of the presence of the triazolyl proton in between two sp^2 and sp^3 nitrogen atoms. In contrast, the triazolyl proton of isomer **21b** appeared at more downfield because of the poor electronic environment generated by the presence of two sp^2 and sp^2 nitrogen atoms.

Evaluation of the antimicrobial and antiquorum-sensing activities

The antimicrobial activities of the synthesized products (Table 1) were assessed *via* measuring the average diameter of the inhibition zones in millimeters (Pearson et al. 1980; Holt 1975). In addition, the minimum inhibition concentrations (MICs, mg/mL) of the most active compounds against the Gram positive bacteria *B. cereus* in addition to the fungal organisms, *C. albicans*, and *A. fumigatus*, were determined by broth microdilution method using 96-multiwell microtiter plates as shown in Table 2 (Andrews 2001). Formylchromone **2** and tetracarbonyl **14** were the most effective against *B. cereus* bacteria with inhibition zone diameters greater than that of the reference antibiotic Ampicillin/Clavulanic acid. Also, these compounds; **2** and **14** were very active to kill 50% of *B. cereus* population with minimum concentration range of 0.002–0.004 mg/mL. In the case of *C. albicans*, however compounds **2**, **5**, **13**, **14**, **16b**, and **17** showed acceptable activities which is less than the reference drugs, the rest compounds were very inactive or non-active at all. In addition, compounds **2**, **11c**, **14**, **16a**, **16b**, and **16c** revealed activities equal to that of amphotericin B against *A. fumigatus* with MIC value of 0.064 mg/mL. Based upon the aforementioned observations, these products might be appropriate candidates for further modifications to achieve potent antimicrobial activities.

Table 1 Antimicrobial and antiquorum-sensing activities

Comp. no.	Inhibition zone diameter (mm)[a,b]			QS inhibition (mm)[c]
	B. cereus	*C. albicans*	*A. fumigatus*	*C. violaceum*
2	15	2	15	6
5	–	2	-	–
6	–	–	–	–
7	–	–	–	–
8	–	–	–	–
11a	–	–	–	–
11b	–	–	–	
11c	12	–	15	3
12	–	–	–	–
13	–	2	–	–
14	15	2	15	7
16a	8	–	15	4
16b	9	2	15	3
16c	–	–	15	–
17	–	2	–	–
18	–	–	–	–
19	–	–	–	–
21	–	–	–	–
Ampicillin/ clavulanic acid	7	–	–	Nt
Fluconazole	nt	3	–	Nt
Amphotericin B	nt	10	15	Nt

nt not tested.

[a]Results after subtraction of DMSO activity

[b]Not active (–, inhibition zone < 2 mm); weak activity (2–9 mm); moderate activity (10–15) mm; strong activity (16–25 mm); very strong activity (26–35 mm)

[c]QS inhibition [Pigment inhibition radius (mm)] = growth and pigment inhibition radius (r_2) − Bacterial growth inhibition radius (r_1).

Table 2 Minimal inhibition concentrations (MICs) of the most active compounds

Comp. no.	MIC (mg/mL)		
	B. cereus	*C. albicans*	*A. fumigatus*
2	0.002	0.512	0.064
5	–	0.265	–
11c	0.008	–	0.064
13	–	0.265	–
14	0.004	0.128	0.064
16a	0.128	–	0.064
16b	0.128	0.265	0.064
16c	–	–	0.064
17	–	0.265	–
Ampicillin/clavulanic acid	0.512	Nt	Nt
Fluconazole	–	0.265	–
Amphotericin B	–	<0.001	0.001

–: means no activity (MIC > 2500 mg/mL).

nt not tested

The quorum sensing inhibitors are promising tools to control the bacterial resistance to antimicrobials and attenuate bacterial virulence (Bhardwaj et al. 2013). Thus, the synthesized compounds were checked for their antiquorum-sensing activity against *C. violaceum* which the violet pigment violacein in response to autoinducer molecules known as acyl HSLs (McClean et al. 1997; Vandeputte et al. 2010; Mohamed et al. 2014). As a result, the compounds that could inhibit acyl HSLs in *C. violaceum* would prevent the purple pigment production. Compounds **2**, **11c**, **14**, **16a**, and **16b** were found to reveal antiquorum-sensing activity (Table 1). Based upon the antimicrobial and the antiquorum-sensing activities, the formylchromone **2** and tetracarbonyl **14** could be good scaffolds to build up potent antibacterial and antifungal agents with high antiquorum-sensing activity.

Computational analysis

Estimation of the pharmacokinetic parameters

The synthesized derivatives were introduced to an in silico ADMET screening using the SwissADME predictor software to calculate the potential ADMET properties of candidate drugs (Table 3). Physicochemical parameters are important to evaluate the molecular transport *via* membrane and therefore, the transport properties of the drug in the blood brain barrier and intestines. These parameters are molecular weight (MW), count of specific atom types (hydrogen donors, hydrogen acceptors and rotatable bonds) and polar surface area (PSA). PSA is calculated using topological polar surface area (TPSA) that represents the surface associated with polar atoms and calculated based on the sum of fragment contributions of *N*- and *O*-centered polar fragments (Daina et al. 2017). Compound **2** possesses no hydrogen atom donors and 3 hydrogen atom acceptors, but compound **14** has one hydrogen atom donor and 5 hydrogen atom acceptors. When the number of rotatable bonds increases, the compound according to Lipinski's rule becomes more adaptable and more flexible for interaction with the binding target. The number of rotatable bonds for compound **2** and **14** are 2 and 4, respectively, simulating better interactions with compound **14**. Physicochemical values clearly indicate that the compounds **2** and **14** can be able to bind the receptor site effectively.

Lipophilicity is described by the partition coefficient between water and *n*-octanol (Log $P = \log$ Po/w) is used to assess the hydrophobicity that affects the drug bioavailability, absorption, drug-receptor interactions, metabolism of molecules, and toxicity. SILICOS-IT is calculated using hybrid method relying on 27 fragments and 7 topological descriptors (http://silicos-it.be.s3-website-eu-west-1.amazonaws.com/). The consensus log Po/w is the arithmetic mean of the Log *P* values predicted by five different proposed methods (Daina et al. 2014). The compounds **2** and **14** have log *P* values found to be below 5, which means these compounds should have good permeability across cell membranes. Water solubility represents one of the important properties which affect drug absorption, as highly water-soluble drugs will deliver a sufficient amount of the drug using small dosage (Savjani et al. 2012). Both compounds (**2** and **14**) are water soluble. Therefore, they will be good candidates for absorption.

Pharmacokinetics prediction will provide the knowledge about the active efflux of the compounds through biological membranes, like the gastrointestinal wall, the lumen, or the brain (Daina and Zoete 2016). The results for absorption of compounds **2** and **14** across gastrointestinal wall and permeability glycoprotein (P-gp) that is an important member between ATP-binding cassette transporters suggested that they will have high active efflux across membranes. Bioactivity score describes the positive medicinal impacts of the putative drugs against a biological target in living organisms. The greater the bioactivity score, the higher probability will be the medicinal impact. Therefore, a compound having bioactivity score above zero is likely to possess higher biological activities in clinical trial stage (Martin 2005). Both compounds have high bioactivity score.

Toxicity assessment by AdmetSAR-2 online predictor is a very important factor to predict whether these new derivatives are toxic or not relying on the carcinogenic, toxigenic and mutagenic activity (Yang et al. 2018). Carcinogenicity represents a type of toxicity, which may cause the growth of cancer in human body. In addition, AMES test predicts the mutagenic activity of the synthesized derivatives. From the toxicity prospective, the compounds **2** and **14** are likely have no toxicity risk.

Prediction of antimicrobial activity using PASS online predictor

PASS online software was used to predict the putative antimicrobial activity spectrum of the synthesized derivatives which is represented in Table 4. The PASS online predictor checks the decomposition of structure in descriptors, and then compare with descriptors of biologically active compounds available in the database. A case of point, this tool provides predictions of biological activities for the synthesized compounds correlating Pa with Pi . Results for the antimicrobial activity prediction illustrated that the synthesized compounds **2** and **14** may show the best antimicrobial (antifungal and antibacterial) activities.

Molecular docking analysis

Molecular docking simulation is used to investigate the drug–target interactions as well as to discover the exact

Table 3 Pharmaceutical prediction of in silico ADMET properties

Compound no.	Molecular formula	Molecular weight (g/mol)	Physico–chemical properties						Bioavailability Score	Water Solubility Silicos-IT class	Pharmacokinetics		Toxicity parameters		
			#Rotatable bonds	#H-bond acceptors	#H-bond donors	TPSA	Lipophilicity	Silicos-IT Log P	Consensus Log P		GI absorption	Pgp substrate	Carcinogens	AMES Mutagenesis	Irritation
2	$C_{17}H_{14}O_3$	266.29	2	3	0	47.28	3.11	2.62	0.55	Soluble	High	+	−	−	−
5	$C_{20}H_{15}N_3O_2$	329.35	4	4	2	100	3.95	3.18	0.55	Poorly soluble	High	−	−	+	−
6	$C_{20}H_{14}N_2O_3$	330.34	1	4	2	90.19	2.35	2.57	0.56	Soluble	High	+	−	−	−
7	$C_{21}H_{15}NO_4$	345.35	3	5	0	68.87	5.87	3.82	0.55	Poorly soluble	High	−	−	+	−
8	$C_{20}H_{13}NO_3S_2$	379.45	3	3	1	116.7	6.4	3.96	0.55	Poorly soluble	High	−	−	−	−
11a	$C_{27}H_{24}O_3$	396.48	3	3	0	39.44	7.09	5.42	0.55	Poorly soluble	High	−	−	−	−
11b	$C_{29}H_{28}O_3$	424.53	3	3	0	39.44	7.55	6.03	0.55	Poorly soluble	Low	−	−	−	−
11c	$C_{33}H_{32}O_5$	508.6	1	5	0	69.67	6.43	5.35	0.55	Poorly soluble	Low	+	−	−	−
12	$C_{26}H_{17}O_4$	393.41	1	4	0	60.44	4.44	3.38	0.55	Moderately soluble	High	+	−	−	−
13	$C_{26}H_{17}NO_3$	391.42	1	4	1	54.37	2.76	3.21	0.56	Soluble	High	+	−	−	−
14	$C_{25}H_{18}O_5$	398.41	4	5	1	88.51	3.64	3.19	0.56	Soluble	High	+	−	−	−
16a Enol−imine	$C_{29}H_{24}N_2O_2$	432.51	3	3	2	53.31	1.54	3.16	0.55	Soluble	High	+	−	+	−
16a Keto −enamine	$C_{29}H_{24}N_2O_2$	432.51	6	2	2	50.36	5.88	5.53	0.55	Insoluble	High	−	−	+	−
16b Enol-imine	$C_{31}H_{28}N_2O_4$	492.57	3	5	2	71.77	1.64	2.9	0.55	Soluble	High	+	−	+	−
16b Keto-enamine	$C_{31}H_{28}N_2O_4$	492.57	8	4	2	68.82	6.02	5.51	0.55	Insoluble	High	−	−	+	−
16c Enol-imine	$C_{27}H_{22}N_4O_2$	434.49	3	5	2	53.31	−1.21	0.75	0.55	Soluble	High	+	−	+	−
16c Keto-enamine	$C_{27}H_{22}N_4O_2$	434.49	6	4	2	76.14	4.73	4.09	0.55	Poorly soluble	High	−	−	+	−
17	$C_{23}H_{16}N_2O_2$	352.39	1	3	1	50.15	1.29	2.01	0.56	Soluble	High	+	−	−	−
18	$C_{31}H_{22}N_2O_2$	454.52	1	3	1	50.15	2.64	3.31	0.56	Moderately soluble	High	+	−	+	−
19	$C_{23}H_{18}N_2O_2$	354.4	5	3	1	55.12	4.7	4.32	0.55	Poorly soluble	High	−	Warning	−	−
20a	$C_{19}H_{14}N_4O_2$	330.34	1	5	1	50.15	−1.45	0.41	0.55	Soluble	High	+	−	+	−
20b	$C_{19}H_{14}N_4O_2$	330.34	1	5	1	50.15	−1.45	0.58	0.55	Soluble	High	+	−	+	−
21a	$C_{19}H_{14}N_4O_2$	330.34	1	5	1	37.3	−1.94	0.54	0.56	Soluble	Low	+	−	+	−
21b	$C_{19}H_{14}N_4O_2$	330.34	1	5	1	37.3	−1.94	0.1	0.56	Soluble	Low	+	−	+	−

TPSA topological polar surface area, *GI* gastrointestinal, *Pgp* permeability glycoprot

Table 4 Antimicrobial activity assessment using PASS online software

Compound no.	Antifungal		Antibacterial	
	Pa	Pi	Pa	Pi
2	0.500	0.321	0.500	0.030
5	0.318	0.074	N/A	N/A
6	N/A	N/A	0.177	0.174
7	0.326	0.071	0.206	0.112
8	0.373	0.056	0.335	0.048
11a	0.364	0.059	N/A	N/A
11b	0.364	0.059	N/A	N/A
11c	0.196	0.139	N/A	N/A
12	0.098	0.072	0.158	0.157
13	0.223	0.123	0.299	0.030
14	0.574	0.330	0.330	0.049
16a Enol-imine	N/A	N/A	0.192	0.126
16a Keto-enamine	0.289	0.088	0.176	0.140
16b Enol-imine	N/A	N/A	0.183	0.134
16b Keto-enamine	0.300	0.081	0.162	0.153
16c Enol-imine	N/A	N/A	N/A	N/A
16c Keto-enamine	0.290	0.087	N/A	N/A
17	N/A	N/A	N/A	N/A
18	N/A	N/A	0.224	0.091
19	0.250	0.107	0.172	0.144
20a	0.267	0.097	0.163	0.152
20b	0.267	0.097	0.163	0.152
21a	0.260	0.101	0.241	0.070
21b	N/A	N/A	N/A	N/A

Pa probability to be active, *Pi* probability to be inactive

binding site to predict the mode of action of the newly synthesized drugs. In this study, the biological targets in the studied bacteria and fungi were predicted in order to define the mechanism of antimicrobial activities for the synthesized derivatives especially formylchromone **2** and tetracarbonyl **14** derivatives.

Penicillin-binding proteins (PBPs); DltA (*D*-alanyl carrier protein ligase) protein, and AlkD DNA glycosylase are the bacterial targets. PBPs are a group of proteins in the bacterial cell wall that are characterized by their affinity and binding of penicillin. Antibacterial compounds inhibit binding of glutamine synthetase to PBPs, which are essential for bacterial cell wall synthesis, resulting in autolysis of the bacterial cells by autolysin enzymes (Dua et al. 2011). DltA protein functions in *D*-alanylation of lipoteichoic acids and modulates the ligand binding and surface charge of Gram-positive cell wall. Disruption of the bacterial dlt operon inhibits the DltA protein and teichoic acid alanylation that render the bacteria more susceptible to antibiotics and host defense responses (Osman et al. 2009). AlkD DNA glycosylases protect bacterial genome integrity

Table 5 Docking scores for protein–ligand interactions of the formylchromone **2** and tetracarbonyl **14** derivatives

Ligand	Compound 2	Compound 14
3TG9	−8.6	−10.1
3FCE	−7.4	−9.1
5KUB	−7.3	−9
4LXJ	−7.9	−10.4
5TZ1	−8.9	−9.4
4UYL	−8.3	−8.3
3N9K	−9.3	−10.1

by detecting and excising aberrant nucleobases. *Bacillus cereus* AlkD is the only DNA glycosylase which catalyzes excision of bases without extruding the damaged nucleotide from the DNA helix. Therefore, disturbance of DNA glycosylase will cause damage of bacterial genome (Parsons et al. 2016).

On the other hand, cytochrome P 450-dependent enzyme 14-steroldemethylase, and 1.3 glucans are the fungal targets. Cytochrome P 450-dependent enzyme 14-steroldemethylase converts lanosterol to ergosterol, that is required in synthesis of fungal cell membrane, and thus inhibition of the enzyme results in inhibition of fungal growth. The beta (1,3)-*D*-glucan is a polysaccharide component of the fungal cell wall which catalyzed by UDP-glucose beta(1,3)-*D*-glucan beta(3)-*D*-glucosyltransferase. Inhibition of the enzyme will block fungal cell-wall synthesis (Dua et al. 2011). Screening of several targets has been done, and the selected targets in Table 5 showed good to very good binding affinities to the compounds **2** and **14**.

For *B. halodurans* penicillin binding protein (PDB ID 3TG9), none of the two compounds (**2** and **14**) make any polar contacts with the protein. Instead, both of them occupy the hydrophobic pocket and are stabilized through numerous van der Waals' interactions with residues. Compound **2** is stabilized through Van der Waals' interactions with LEU-201, LEU-195, ASN-36, ARG-37, ALA-197, ILE-41, ASP-193, THR-194, ALA-38, THR-213, ALA-200 (Fig. 2a, b). Compound **14** is stabilized through Van der Waals' interactions with PHE-115, PHE-107, ALA-54, ASP-293, GLY-228, SER-55 (Fig. 2c, d).

For lanosterol 14-*alpha* demethylase from *S. cerevisiae* (PDB ID 4LXJ), the two compounds **2** and **14** show identical binding modes that involve polar interactions with the protein. Compound **2** has polar interactions with ASP-233 residue (Fig. 2e, f), and compound **14** has polar interactions with ARG-98 and ALA-69 residues (Fig. 2g, h). In both cases, the ring containing the heteroatom (Formylchromone **2** and tetracarbonyl **14**) is stabilized through Van der Waals' interactions with TYR-229, ALA-226, ILE-205, LEU-221,

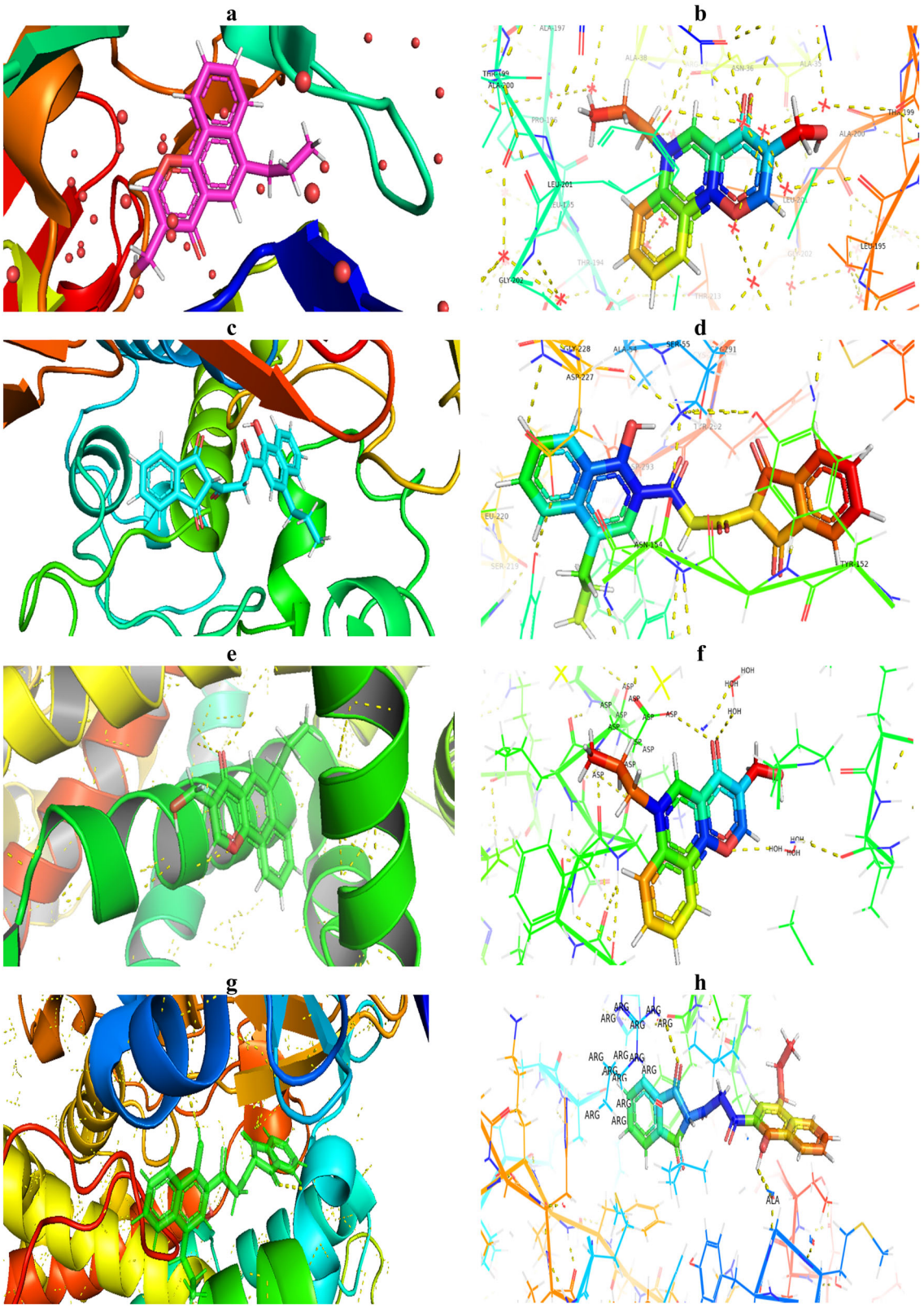

Fig. 2 Molecular docked models for formylchromone **2** and tetracarbonyl **14** derivatives; **a**, **b** 3TG9-Compound **2**; **c**, **d** 3TG9-Compound **14**; **e**, **f** 4LXJ-Compound **2**; **g**, **h** 4LXJ-Compound **14**

GLN-316, PRO-201 in case of compound **2**, and VAL-242, LEU-96, LEU-95, ILE-293, GLY-73, PHE-241, PHE-384, ALA-125 in compound **14**. Collectively, molecular docking simulations suggested that the formylchromone **2** and tetracarbonyl **14** ligands have substantial antimicrobial activity.

Conclusion

A convenient protocol for the synthesis of new angular chromones bearing allylnaphthyl fragment has been reported. The precursor 6-allyl-3-formyl-4*H*-benzo[*h*]chromone (**2**) was prepared *via* Vilsmeier–Haack reaction of 4-allyl-1-hydroxy-2-acetonaphthone (**1**), which was subsequently reacted with different active methylene-based reagents, amines, and others to build up different isolated and condensed heterocyclic compounds. The antimicrobial and antiquorum-sensing activities of the newly synthesized compounds showed that many compounds have good and promising activities in comparison with the reference drugs. The formylchromone **2** and tetracarbonyl **14** showed the best antibacterial and antifungal activities in addition to promising antiquorum-sensing activity. Based on the skeletal keys of formyl chromone **2** and tetracarbonyl **14**, further synthetic studies to realize potent antibacterial and antifungal agents with high antiquorumsensing activity are currently underway and will be reported in the due time. Computational prediction of pharmacokinetics, drug-likeness properties, biological activity, and molecular docking suggested that formyl chromone **2** and tetracarbonyl **14** may be potent antimicrobial drugs.

Compliance with ethical standards

Conflict of interest The authors declare that they have no conflict of interest.

Publisher's note: Springer Nature remains neutral with regard to jurisdictional claims in published maps and institutional affiliations.

References

Abdel-Rahman SA, El-Gohary NS, El-Bendary ER, El-Ashry SM, Shaaban MI (2017) Synthesis, antimicrobial, antiquorum-sensing, antitumor and cytotoxic activities of new series of cyclopenta (hepta)[*b*]thiophene and fused cyclohepta[*b*]thiophene analogs. Eur J Med Chem 140:200–211

Andrews JM (2001) Determination of minimum inhibitory concentrations. J Antimicrob Chemother 48:5–16

Bhardwaj AK, Vinothkumar K, Rajpara N (2013) Bacterial quorum sensing inhibitors: attractive alternatives for control of infectious pathogens showing multiple drug resistance. Recent Pat Anti-infect Drug Discov 8:68–83

Daina A, Zoete V (2016) A BOILED-egg to predict gastrointestinal absorption and brain penetration of small molecules. Chem Med Chem 11:1117–1121

Daina A, Michielin O, Zoete V (2014) iLOGP: a simple, robust, and efficient description of *n*-octanol/water partition coefficient for drug design using the GB/SA approach. J Chem Inf Model 54:3284–3301

Daina A, Michielin O, Zoete V (2017) SwissADME: a free web tool to evaluate pharmacokinetics, drug-likeness and medicinal chemistry friendliness of small molecules. Sci Rep 7:42717

Dua R, Shrivastava S, Sonwane SK, Srivastava SK (2011) Pharmacological significance of synthetic heterocycles scaffold: a review. Adv Biol Res 5:120–144

El-Desoky SI, Keshk EM, El-Sawi AA, Abozeid MA, Abouzeid LA, Abdel-Rahman ARH (2018) Synthesis, biological evaluation and in silico molecular docking of novel 1-hydroxy-naphthyl substituted heterocycles. Saudi Pharm J 26:852–859

Ellis GP (1977) Chromenes, chromanones and chromones. John Willy & Sons, New York

Ghosh CK, Khan S (1981) Heterocyclic systems; 10^1. Defunct 4-oxo-4*H*-[1] benzopyran-3-carboxylic acids -3-carboxaldehydes. Synthesis 1981:719–721

Holt RJ (1975) Laboratory tests of antifungal drugs. J Clini Pathol 28:767–774

Karad SC, Purohit VB, Thummar RP, Vaghasiya BK, Kamani RD, Thakor P, Raval DK (2017) Synthesis and biological screening of novel 2-morpholinoquinoline nucleus clubbed with 1,2,4-oxadiazole motifs. Eur J Med Chem 126:894–909

Martin YC (2005) A bioavailability score. J Med Chem 48:3164–3170

McClean R, Pierson LS, Fuqua C (2004) A simple screening protocol for the identification of quorum signal antagonists. J Microbiol Methods 58:351–360

McClean KH, Winson MK, Fish L, Taylor A, Chhabra SR, Camara M, Stewart GS (1997) Quorum sensing and chromobacterium violaceum: exploitation of violacein production and inhibition for the detection of *N*-acylhomoserine lactones. Microbiology 143:3703–3711

Mohamed GA, Ibrahim SR, Shaaban MI, Ross SA (2014) Mangostanaxanthones I and II, new xanthones from the pericarp of *Garcinia mangostana*. Fitoterapia 98:215–221

Osman KT, Du L, He Y, Luo Y (2009) Crystal structure of *Bacillus cereus D*-alanyl carrier protein ligase (DltA) in complex with ATP. J Mol Biol 388:345–355

Parasuraman S (2011) Prediction of activity spectra for substances. J Pharm Pharm 2:52–53

Parsons ZD, Bland JM, Mullins EA, Eichman BF (2016) A catalytic role for C–H/π interactions in base excision repair by *Bacillus cereus* DNA glycosylase AlkD. J Am Chem Soc 138:11485–11488

Pearson RD, Steigbigel RT, Davis HT, Chapman SW (1980) Method of reliable determination of minimal lethal antibiotic concentrations. Antimicrob Agents Chemother 18:699–708

Rex JH, Alexander BD, Andes D, Arthington-Skaggs B, Brown SD, Chaturvedi V, Ghannoum MA, Espinel-Ingroff A, Knapp CC, Ostrosky-Zeichner L, Pfaller MA, Sheehan DJ, Walsh TJ (2008) Reference method for Broth dilution antifungal susceptibility testing of yeasts; approved standard-third edition. Clinical and Laboratory Standards Institute. CLSI document M27-A3

Rex JH, Alexander BD, Andes D, Arthington-Skaggs B, Brown SD, Chaturveli V, Espinel-Ingroff A, Ghannoum MA, Knapp CC, Motyl MR, Ostrosky-Zeichner L, Pfaller M, Sheehan DJ, Walsh TJ (2008) Reference method for Broth dilution antifungal susceptibility testing of filamentous fungi; approved standard-second edition. Clinical and Laboratory Standards Institute. CLSI document M38-A2

Risitano F, Grassi G, Foti F (2001) Reactions of 3-substituted chromones with ortho-phenylenediamine. J Heterocycl Chem 38:1083–1086

Rodríguez M, Santillan R, López Y, Farfán N, Barba V, Nakatani K, García Baéz EV, Padilla-Martinez II (2007) N–H…O Assisted structural change sinduced on ketoenamine systems. Supramol Chem 19:641–653

Sapariya NH, Vaghasiya BK, Thummar RP, Kamani RD, Patel KH, Thakor P, Thakkar SS, Ray A, Raval DK (2017) Synthesis, characterization, in silico molecular docking study and biological evaluation of a 5-(phenylthio) pyrazole based polyhydroquinoline core moiety. New J Chem 41:10686–10694

Savjani KT, Gajjar AK, Savjani JK (2012). Drug solubility: importance and enhancement techniques. ISRN pharm. 2012: Article ID 195727

Sigg I, Haas G, Winkler T (1982) The reaction of 3-formylchromone with *ortho*-substituted anilines. Preparation of a tetraaza[14] annulene. Helv Chim Acta 65:275–279

Thakkar SS, Thakor P, Ray A, Doshi H, Thakkar VR (2017) Benzothiazole analogues: synthesis, characterization, MO calculations with PM6 and DFT, in silico studies and in vitro antimalarial as DHFR inhibitors and antimicrobial activities. Bioorg Med Chem 25:5396–5406

Trott O, Olson AJ (2010) AutoDock vina: improving the speed and accuracy of docking with a new scoring function, efficient optimization, and multithreading. J Comput Chem 31:455–461

Vandeputte OM, Kiendrebeogo M, Rajaonson S, Diallo B, Mol A, El Jaziri M, Baucher M (2010) Identification of catechin as one of the flavonoids from *Combretum albiflorum* bark extract that reduces the production of quorum-sensing-controlled virulence factors in *Pseudomonas aeruginosa* PAO1. Appl Environ Microbiol 76:243–253

Patel JB, Cockerill FR, Bradford PA, Eliopoulos GM, Hindler JA, Jenkins SG, Lewis JS, Limbago B, Miller LA, Nicolau DP, Powell M, Swenson JM, Traczewski MM, Turnidge JD, Weinstein MP, Zimmer BL (2015) Performance standards for antimicrobial susceptibility testing; 25th informational supplement. CLSI document M100-S25. Clinical and Laboratory Standards Institute, Wayne

Yahiaoui S, Fagnere C, Pouget C, Buxeraud J, Chulia AJ (2008) New 7, 8-benzoflavanones as potent aromatase inhibitors: synthesis and biological evaluation. Bioorg Med Chem 16:1474–1480

Yang H, Lou C, Sun L, Li J, Cai Y, Wang Z, Tang Y (2018) admetSAR 2.0: web-service for prediction and optimization of chemical ADMET properties. Bioinformatics 35:1067–1069